Molecular Catalysis 529 (2022) 112531

Contents lists available at ScienceDirect

Molecular Catalysis

journal homepage: www.journals.elsevier.com/molecular-catalysis

Testing the role of the backbone length using bidentate and tridentate ligands in manganese-catalyzed asymmetric hydrogenation

Zsófia Császár [a], Regina Kovács [a], Máté Fonyó [a], József Simon [b], Attila Bényei [c], György Lendvay [d,e], József Bakos [a], Gergely Farkas [a,*]

[a] Research Group of Organic Chemistry – Synthesis and Catalysis, University of Pannonia, Egyetem u. 10, H-8200 Veszprém, Hungary
[b] Research Group of Analytical Chemistry, University of Pannonia, Egyetem u. 10, H-8200 Veszprém, Hungary
[c] Department of Physical Chemistry, University of Debrecen, Egyetem tér 1, H-4032 Debrecen, Hungary
[d] Institute of Materials and Environmental Chemistry, Hungarian Academy of Sciences, Magyar tudósok krt. 2., H-1117 Budapest, Hungary
[e] Department of General and Inorganic Chemistry, University of Pannonia, Egyetem u. 10, H-8200 Veszprém, Hungary

ARTICLE INFO

Keywords:
Asymmetric hydrogenation
Manganese
Bidentate and tridentate ligand
Earth abundant metal

ABSTRACT

Manganese complexes modified by simple alkane-diyl based P,N ($Ph_2PCH(CH_3)(CH_2)_mCH(CH_3)NHC_2H_5$; $m = 0$, 1) and potentially tridentate P,N,N ($Ph_2PCH(CH_3)(CH_2)_mCH(CH_3)NH(CH_2)_nN(CH_3)_2$; $m = 0$, 1; $n = 2$, 3) type ligands have been synthesized and tested in the asymmetric hydrogenation of ketones. The combined coordination and catalytic studies led to the conclusion that the N-N tether length of the P,N,N type compounds plays a crucial role in determining the chemoselectivity, while the length of the P-N skeleton has been shown to affect the catalytic activity. Mn-catalysts containing P,N,N ligands with the proper tether lengths ($m = 0$, $n = 1$) provided high enantioselectivities (up to 95% *ee*) and activities in the asymmetric hydrogenation of acetophenone derivatives. The influence of substitution of the acetophenone substrate and the reaction conditions is demonstrated. Based on quantum chemistry calculations, a qualitative model explaining the origin of enantioselectivity is proposed.

1. Introduction

Transition-metal catalyzed asymmetric hydrogenation of prochiral ketones represents one of the simplest and most convenient chemical transformations producing optically active secondary alcohols that serve as valuable building blocks for biologically active compounds such as medicines, fragrances and agrochemicals [1,2,3,4]. Over the past decades noble-metal catalysts, especially Ru, Ir and Rh complexes have been utilized in those transformations providing extremely high efficiency [5]. In recent years, however, a remarkable progress has been devoted to replace noble metal catalyst with earth-abundant, less expensive, and less toxic transition metals, like iron, cobalt, copper, nickel or manganese [6,7,8]. Amongst these examples, chiral manganese-complexes proved to be a particularly valuable class of catalysts [9,10,11] due to their high activity [12], the biocompatibility of the metal and the sustainable nature of its production.

Although manganese-catalyzed asymmetric hydrogenation is a relatively young research area, in the last few years a number of catalytic systems have been developed in the field. Indeed, the pioneering work of Kirchner [13], Beller [14] and Clarke [15] opened up new avenues in the synthesis and catalytic application of chiral Mn-complexes in the area of both asymmetric direct (ADH) and transfer hydrogenation (ATH) reactions. Besides simple aryl alkyl ketones [16,17,18], α,β-conjugated carbonyl compounds [19], unsymmetrical benzophenones [20], α-substituted-β-ketoamides [21] and quinoline-derivatives [22] were also successfully converted to the desired chiral products with high enantioselectivity and activity using novel Mn-catalysts. Although in several cases bidentate [23,24,25] and macrocyclic polydentate [26] (P_xN_y, where $x+y > 3$) ligands were found as efficient chiral selectors, the field is basically dominated by catalytic systems containing tridentate P,N,N or P,N,P type ligands (Fig. 1).

The structural modularity of the latter ligand classes as well as the synthetic strategies available for their preparation facilitate stereoelectronic fine-tuning that, in many cases, led to improved catalytic performance. Clarke and coworkers argued that the use of electron donating phosphine moiety (Ar = 4-MeO-3,5-Me_2-phenyl) together with an electron-rich pyridine unit (R = NMe_2 in the 4-position) results in considerable increase in the hydrogenation reaction rate compared to

* Corresponding author:
E-mail address: gerifarkas@almos.uni-pannon.hu (G. Farkas).

https://doi.org/10.1016/j.mcat.2022.112531

Available online 28 July 2022

the ligand with less electron-rich moieties (Ar = Ph, R = H) [27]. Ding et al. also demonstrated that the substituent controlled fine-tuning of the donoratoms in lutidine-based chiral manganese complexes can be used to enhance catalytic activity and enantioselectivity [28]. The catalyst with properly tuned structure (R^1 = *t*Bu, R^2 = *i*Pr) provided chiral alcohols with excellent turnover (TON up to 9800) and optical yield (*ee* up to 98%). Morris and coworkers found that a P,N,N ligand with a rather rigid phenylene-based P-N skeleton forms a cationic complex with *fac* stereochemistry, unlike the analogous ethylene-bridged compound that produces a neutral *mer* isomer in the reaction with $Mn(CO)_5Br$ [29]. Furthermore, while the former Mn-catalysts proved to be inactive in the ATH of acetophenone, the latter provided full conversion under identical reaction conditions.

The ligand family developed by Zhong [20] and Liu [22] et al. highlighted the importance of steric characteristics of the terminal ligand substituents. Manganese catalysts modified by these ligands afforded impressive turnover numbers and enantioselectivities in the asymmetric hydrogenation of unsymmetrical benzophenones (TON up to 13000, *ee* up to >99%) and in the enantioselective reduction of quinolines (TON up to 3840, *ee* up to 97%). In an excellent study, Zhang and coworkers designed P,N,P ligands capable of forming 5- and 7-membered fused chelate structures [30]. It has been found that the interplay between the flexible 5-membered and the rigid 7-membered rings leads to effective enantiomeric discrimination in the hydride transfer step. The success of the strategy has been demonstrated in the ADH of a large number of ketones with excellent selectivity and stability (*ee*s 92-99% for aryl alkyl ketones, TON up to 2000).

These examples (summarized in Fig. 1) clearly show that the ligand modifications have usually followed the principle of altering simply the spatial demands of the catalyst, and/or substituent controlled electronic tuning of the donor N or P atoms. To the best of our knowledge, however, the systematic variation of the length of the ligand's backbone determining the chelate ring size has not yet been investigated for such systems. As a matter of fact, this type of study is extremely rare concerning tridentate ligands in transition metal catalysis [31,32,33,34,35], especially in asymmetric catalysis, although changes in tether length can readily be implemented resulting in steric and also electronic alteration of the catalyst which can lead to dramatic improvements in catalytic activity and selectivity. The systematic variation of the length of the P-N and N-N backbones can also be considered as a useful combinatorial strategy to find the matching structural elements of ligands by the simultaneous screening of a broad range of stereo-electronic attributes.

Based on this philosophy in ligand design, we report on the synthesis, coordination chemistry and catalytic application of novel Mn(I)-complexes modified by bidentate P,N or potentially tridentate P,N,N type chiral ligands of different P-N and N-N tether length. The coordination properties of the ligands in the octahedral manganese-complexes were analyzed by X-ray crystallography, NMR and IR spectroscopy. The complexes were utilized in the enantioselective hydrogenation of ketonic substrates with the intention to investigate the effect of the P-N and N-N bridge lengths, the substitution pattern of the substrate and the reaction conditions on the activity and enantioselectivity of the catalytic reaction.

2. Results and discussion

2.1. Synthesis and characterization of the catalysts

Recently, we have developed a modular synthetic approach for the preparation of chiral P,N and P,N,N ligands **L2**-**L6** by the nucleophilic ring opening of cyclic sulfates with diamines (Fig. 2) [36,37]. The two-step synthetic procedure enabled the synthesis of potentially tridentate ligands having different P,N and N,N tether length in high yields using commercially available starting materials. In the present study we extended this ligand scope by the synthesis of bidentate P,N compound **L1** using the same synthetic procedure.

Coordination of the ligands to Mn(I) was accomplished by the treatment of the free ligand with 1 molar equivalent of $[Mn(CO)_5Br]$ in toluene at 90°C for 3 h. The solvent was then removed in vacuo and the remaining solid was washed with ether and pentane to give the yellow complexes in high yields. The analysis of the new manganese compounds by IR and NMR spectroscopy enabled the determination of their structure with high confidence (Table 1). Although the resonances of the complexes are often broad giving rise to unresolved NMR signals due to the quadrupole moment of ^{55}Mn, the corresponding $^3J(P,H)$, $^3J(P,C)$ or $^3J(H,H)$ coupling constants could be determined in most cases. These data in combination with 2D NOESY spectra provided valuable information on the preferred chelate conformation of the complexes.

The coordination of bidentate ligands **L1** and **L4** yielded neutral octahedral tricarbonyl chelate complexes $[Mn(\mathbf{L1})(CO)_3Br]$ (**Mn-1**) and

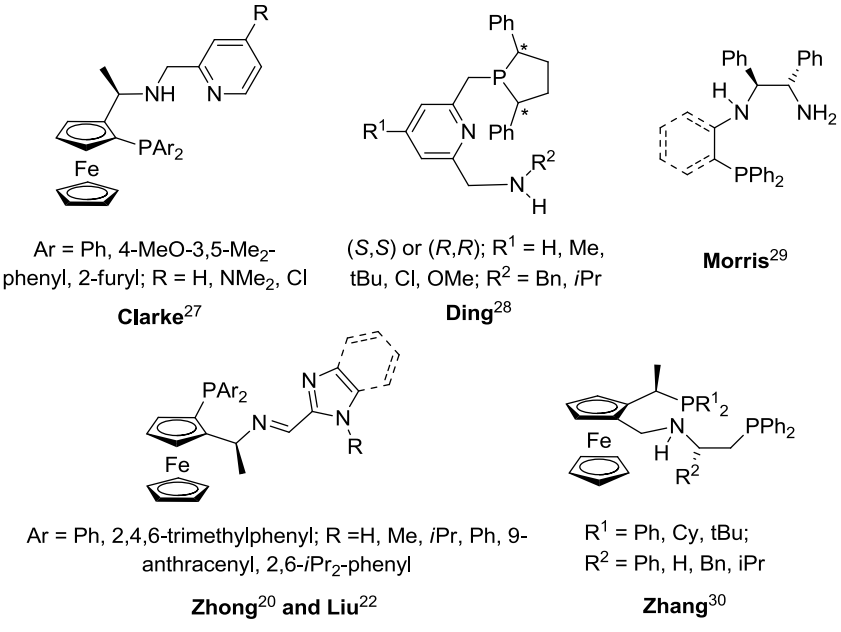

Fig. 1. Representative examples of ligand modifications in Mn-catalyzed asymmetric hydrogenation

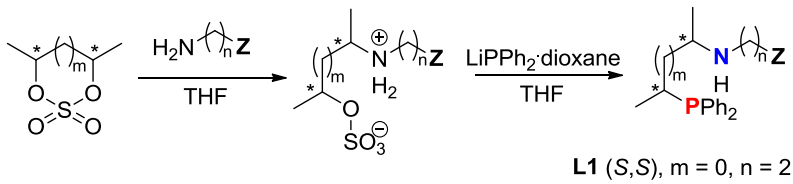

L1 (*S*,*S*), m = 0, n = 2, Z = H
L2 (*S*,*S*), m = 0, n = 2, Z = NMe_2
L3 (*R*,*R*), m = 0, n = 3, Z = NMe_2
L4 (*S*,*S*), m = 1, n = 2, Z = H
L5 (*R*,*R*), m = 1, n = 2, Z = NMe_2
L6 (*S*,*S*), m = 1, n = 3, Z = NMe_2

Fig. 2. Synthesis of chiral ligands L1-L6

Table 1
Spectroscopic (IR and NMR) data and isomeric composition of manganese complexes formed by ligands L1-L6

Complex	Composition	IR, ν(CO) [cm^{-1}] [a]	^{31}P NMR, δ [ppm] [b]
Mn-1	[Mn(**L1**)$(CO)_3$Br]	1897, 1932, 2016	70.8 (93), 65.6 (7)
Mn-2	[Mn(**L2**)$(CO)_2$Br]	1834, 1914	99.6 (70), 100.5 (18), 92.3 (12)
Mn-3	[Mn(**L3**)$(CO)_3$Br]	1896, 1933, 2014	73.0 (80), 67.7 (20)
Mn-4	[Mn(**L4**)$(CO)_3$Br]	1897, 1936, 2018	40.0 (84), 57.2 (16)
Mn-5	[Mn(**L5**)$(CO)_2$Br]	1830, 1919	89.9 (100)
Mn-6	[Mn(**L6**)$(CO)_3$Br]	1893, 1933, 2015	39.3 (78), 38.7 (16), 56.2 (6)

[a] IR spectra were recorded using KBr pellets.
[b] NMR spectra were recorded in CD_2Cl_2 as solvent. Numbers in brackets represent the % ratio of the corresponding isomer based on ^{31}P NMR.

[Mn(**L4**)$(CO)_3$Br] (**Mn-4**), respectively, with facially arranged carbonyl ligands in the coordination sphere. From the IR spectra it is obvious as they show three strong CO bands of similar intensity in agreement with the previously reported P,N ligated Mn(I) complexes (Table 1), [23,24,38].

Additionally, a single crystal, suitable for X-ray structure determination, could be grown by the slow evaporation of the solvent from the solution of **Mn-1** in acetone. The X-ray structure supports, in all respects, the conclusions drawn from the IR analysis (Fig. 4). The P,N chelate ring is stabilized in a δ-skew conformation with equatorially disposed methyl substituents in the backbone. The stereogenic nitrogen atom coordinates with (*R*) absolute configuration, directing the N-H into axial position, *cis* to the Br ligand.

Complexes **Mn-1** and **Mn-4** were investigated in solution by ^1H, $^{13}C\{^1H\}$, $^{31}P\{^1H\}$, ^1H-^1H-COSY, ^1H-^1H NOESY and ^1H-^{13}C HSQC NMR methods using CD_2Cl_2 as solvent. According to the NMR data, two diastereomeric forms of **Mn-1** can be found in solution in a molar ratio of 93:7 (Table 1). For the major isomer, the ^1H and ^{13}C resonances can be fully assigned that has the same ring conformation and nitrogen configuration as was found by the single crystal X-ray diffraction in the solid phase. It can be deduced using the characteristic NOE cross peaks and the $^{13}C\{^1H\}$ NMR spectrum. The relatively large coupling (close to the Karplus maximum) [39] between the phosphorus and the methyl carbon adjacent to the nitrogen ($^3J(P,C_{Me(CHN)})$ = 13.5 Hz), suggests the P-C-C-C_{Me} torsion angle to be large (~180°), and therefore the equatorial position of this methyl substituent (Fig. 5, **I**). The minor isomer may differ in (i) the nitrogen configuration, (ii) the relative position of the N-H and the Br ligand, or (iii) in the ring conformation. Fortunately, the C*H*N methine signal of the *minor* isomer exhibiting a large coupling to phosphorus ($^3J(P,H)$ = ~26 Hz) could straightforwardly be assigned. This coupling pattern is only possible in a λ-skew conformation with axially disposed methyl substituents (Fig. 5, **II**). Similarly to the Mn-complex of **L1**, **Mn-4** containing a six-membered chelate ring exists in solution as a mixture of two isomers in a molar ratio of 86:14 (Table 1).

A different coordination pattern has been observed for ligands **L2** and **L5** with dimethylaminoethyl side chain. At first, only two high intensity C=O stretching bands appear in their IR spectra (Table 1). Again, the number and positions of these bands are particularly informative about the structure of the complexes and strongly suggest the *meridional* coordination of the P,N,N ligand, in a tridentate fashion, resulting in the formation of neutral dicarbonyl Mn-complexes (Fig. 3) [29,40,41]. The tridentate coordination mode was also evidenced by ^{31}P and ^1H NMR spectroscopy. The methyl signals of the dimethylamino moiety appeared as two singlets as the two CH_3 groups became diastereotopic upon coordination. Compound [Mn(**L2**)$(CO)_2$Br] (**Mn-2**) is present as a mixture of three isomers in a ratio of 70:18:12 in CD_2Cl_2 solution according to NMR spectroscopy (Table 1). The P,N chelate ring in the *major* component adopts a skew conformation with equatorial methyl groups as indicated by the relatively large $^3J(P,C)$ coupling constants between the phosphorus and the backbone methyl carbon adjacent to the nitrogen ($^3J(P,C_{Me(CHN)})$ = 12.4 Hz), similarly to the major isomer of **Mn-1**. Furthermore, the strong NOE interaction between the NH and the axially disposed CHP hydrogen suggests the coordination of the nitrogen with (*R*) configuration (Fig. 5, **I**). Unfortunately, the exact identification of the *minor* components was not possible due to their low concentration and signal overlapping. It is, however, reasonable to assume that they differ from the *major* isomer in the manganese and/or nitrogen configuration. Complex [Mn(**L5**)$(CO)_2$Br] (**Mn-5**) is present in solution as a single diastereomer. Based on the characteristic NOE interactions (e.g. between C*H*$_3$(CHP) and C*H*N hydrogens) it is assumed that the P,N ring is stabilized in a chair conformation with axial-equatorial backbone methyl substituents moving from the phosphorus towards the nitrogen

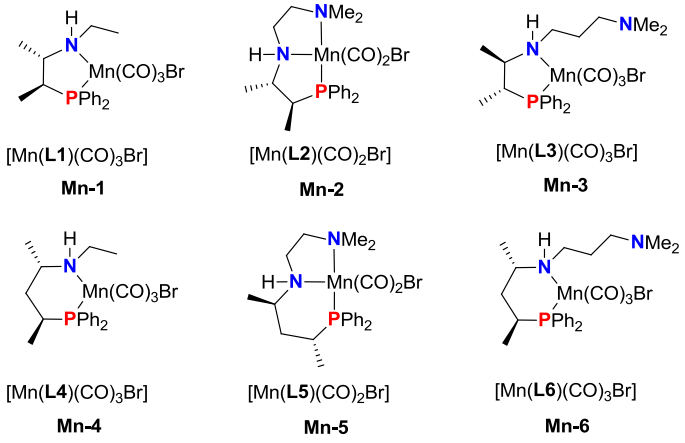

Fig. 3. Manganese(I) complexes formed by ligands L1-L6

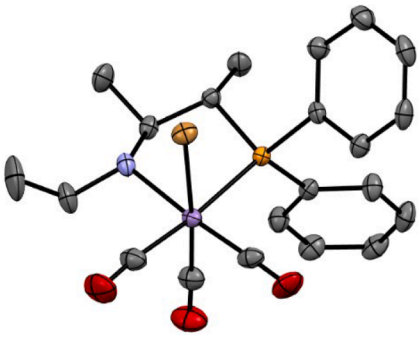

Fig. 4. ORTEP diagram of Mn-1 (thermal ellipsoids are shown at 30 % probability level, hydrogen atoms have been omitted for clarity)

along the ligand backbone (Fig. 5, **III**).

Complexes [Mn(**L3**)$(CO)_3$Br] (**Mn-3**) and [Mn(**L6**)$(CO)_3$Br] (**Mn-6**) exist in solution as mixtures of isomers. Interestingly, compounds **L3** and **L6** coordinate as bidentate P,N ligands. Their non-coordinating dimethylaminopropyl moiety appears as a pendant side arm, that is evidenced by the close similarity of their ^{1}H and ^{31}P chemical shifts and coupling constants to those of complexes formed by bidentate ligands **L1** and **L4**, respectively. Additionally, the $N(CH_3)_2$ moiety appeared as a singlet in the ^{1}H NMR spectra without noticeable deshielding of the methyl signals compared to the free ligand. Most importantly, the IR spectra of complexes **Mn-3** and **Mn-6** showed the same number of C=O stretching bands at almost the same positions as for complexes containing bidentate ligands **L1** and **L4**, respectively. Based on the above experimental evidences it can be deduced that the N-N tether length of P,N,N ligands strongly affects coordination behavior. Only five-membered N,N chelate rings could be observed, the formation of rings with larger size can be considered to be unfavored.

2.2. Catalytic studies

2.2.1. Screening of the catalysts

With the Mn-catalysts **Mn-1-Mn-6** in hand, we set out to evaluate their activity and enantioselectivity in the asymmetric hydrogenation of simple ketones. Initially, the preformed chiral Mn(I)-complexes were applied under direct hydrogenation conditions using acetophenone (**S1**) as substrate and potassium *tert*-butoxide as base in ethanol at a substrate/catalyst (S/C) molar ratio of 100 (Table 2). It has been found that catalysts with ligands coordinating in a bidentate fashion ([Mn(**L**)$(CO)_3$Br], **Mn-1, Mn-3, Mn-4** and **Mn-6**) display considerably lower activity and enantioselectivity. Six-membered chelates of **L4** and **L6** provided no catalytic activity (entries 4 and 6). Surprisingly, in addition to the hydrogenation of **S1**, the five-membered chelates **Mn-1** and **Mn-3** also promoted the formation of butyrophenone, the α-ethylated derivative of the substrate (entries 1 and 3). The mechanism of this alkylation process possibly involves transition metal catalyzed dehydrogenation of solvent ethanol to acetaldehyde, which subsequently undergoes a base-catalyzed condensation with the ketone to yield the corresponding α,β-unsaturated carbonyl compound. In the final step, the 1,4-hydrogenation of the conjugated system affords the C-alkylated ketone [42,43].

Catalysts modified by chiral tridentate ligands **L2** and **L5** provided the hydrogenation product chemoselectively with good enantioselectivity (entries 2 and 5 in Table 2). Similarly to the catalysts having a bidentate ligand [Mn(**L**)$(CO)_3$Br], the size of the P,N chelate ring seems to be an important factor in determining catalytic activity. Chiral complex **Mn-2** having five-membered P,N chelate ring provided higher catalytic turnover (>99% conv.) compared to its analogue with six-membered P,N chelate (74% conv.). Although with some lower activity, **Mn-2** could also be utilized in toluene and in 96 V/V% ethanol as

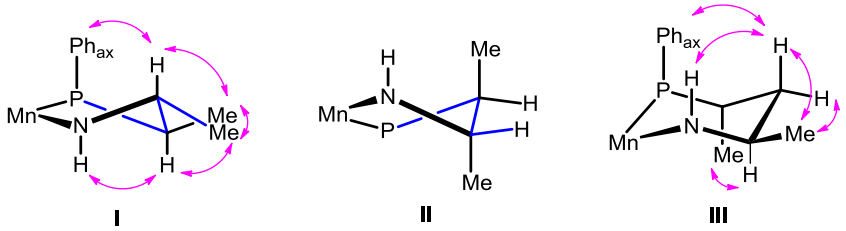

Fig. 5. haracteristic P,N chelate conformations found in the solution of Mn-complexes (pink arrows represent NOE interactions)

Table 2
Mn-catalyzed asymmetric direct hydrogenation of acetophenone: screening of the catalysts[a]

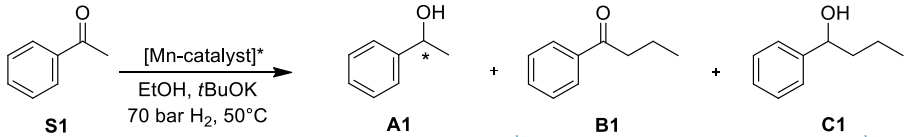

S1 A1 B1 C1

Entry	Catalyst	Conversion (%)[b]	**A1:B1:C1** molar ratio (%)[b]	*Ee* of **A1** (%)[c]
1	**Mn-1**	72	38:51:11	10 (*R*)
2	**Mn-2**	>99	100:0:0	80 (*S*)
3	**Mn-3**	76	55:35:10	6 (*R*)
4	**Mn-4**	0	-	-
5	**Mn-5**	74	100:0:0	82 (*R*)
6	**Mn-6**	0	-	-
7[d]	**Mn-1**	91	100:0:0	12 (*S*)
8[d]	**Mn-2**	51	100:0:0	88 (*S*)
9[e]	**Mn-2**	59	100:0:0	80 (*S*)
10[f]	**Mn-2**	>99	100:0:0	80 (*S*)

[a] Reaction conditions: Catalyst: 0.006 mmol, acetophenone: 0.6 mmol, *t*BuOK: 0.03 mmol, EtOH: 1 ml, temperature: 50°C, H_2 pressure: 70 bar, reaction time: 20h.
[b] Conversion and chemoselectivity were determined by GC using undecane as internal standard.
[c] The *ee* was determined by chiral GC.
[d] Toluene is used as solvent. [e]96% EtOH is used as solvent. [f]*i*PrOH is used as solvent.

solvents (entries 8-10).

In the next set of experiments, Mn-catalysts were screened under transfer hydrogenation (ATH) conditions using *i*PrOH as hydrogen source at a substrate/catalyst molar ratio of 100 (Table 3). Catalytic turnover could only be achieved with catalysts having a five-membered P,N chelate ring (entries 1-3). Catalysts containing bidentate ligands **L1** and **L3** afforded commensurate conversions and enantioselectivities. In addition to *i*PrOH, complex **Mn-1** was tested in ethanol (entry 7). The reaction provided products **A1, B1** and **C1** in a molar ratio of 42:44:14, respectively. The same way, **Mn-2** was also tested in ethanol to assess its ability for the utilization of this solvent as a hydrogen source. In contrast to **Mn-1** having bidentate P,N ligand, **Mn-2** containing tridentate P,N,N system was totally inactive under these conditions.

These findings clearly indicate that in ADH reactions Mn-complexes modified by tridentate ligands are active and enantioselective catalysts, while for transfer hydrogenation reactions catalysts with bidentate ligands work better. Consequently, the N-N tether length studied in this contribution is found to have a remarkable effect on the reactivity pattern of Mn-catalysts. Besides the length of the N-N bridge, the size of the P-N chelate ring also strongly affects the catalytic features: the increase in the P,N ring size has a detrimental effect on activity regardless of the nature of catalysis (i.e. direct or transfer hydrogenation). Similar trends can be extracted from sporadic literature data concerning the effect of ring size on activity of bifunctional catalysts [25,44,45]. Although the exact explanation for the rather distinct catalytic behavior observed for catalysts of different P-N tether length is currently unknown, several factors can be mentioned influencing reactivity. It is surmised that the more pronounced puckering and larger bite angle of the six-membered chelate ring compared to the five-membered system creates a significantly different steric and also electronic environment in the catalyst [46]. Furthermore, the variation of chelate ring size can also give rise to different non-bonding interactions [47].

In addition to these effects, the basicity of the donoratoms must also be taken into account as it can also change due to the variation of the tether length. In order to compare the σ-donor ability of the phosphorus atoms connected to butane-2,3-diyl or pentane-2,4-diyl frameworks the phosphine-selenides of ligands **L1** and **L4** were prepared in the reaction of the free ligand and elemental selenium. The magnitude of the ^{1}J (^{77}Se-^{31}P) coupling constant is very much dependent on the electronic properties of the phosphorus-substituents as electron-withdrawing groups cause it to increase whereas electron-donating substituents reduce its value [48]. Interestingly, only a marginal difference [49] between the $^{1}J(^{77}\text{Se}\text{-}^{31}\text{P})$ coupling constants in selenides of ligands **L1** and **L4** (743.8 and 744.6 Hz, respectively) could be observed indicating that the length of the chiral backbone does not significantly affect the electron-donating ability of its donoratoms.

The distinct catalytic behavior of complexes **Mn-1**-**Mn-6** having different P-N and/or N-N tether length can also be evaluated on the basis of the possible difference in ligands' hemilability. Polydentate ligands featuring a combination of strong and weak coordinating functionalities (eg. P,N,N ligands with soft phosphorus and hard nitrogen donoratoms) can frequently undergo coordination/decoordination processes, that may occur even under catalytic conditions [50]. In pincer complexes usually the lability of only one out of the three donors can be observed, so the metal remains firmly held by the chelate effect in the hemi-dissociated complex. In contrast to this, the decoordination of the weakly bound donor in simple chelates can make the complex vulnerable to further dissociation that may lead to the destabilization of the catalyst [51]. As was found for complexes **Mn-1**-**Mn-6** the formation of six-membered chelate rings is less favoured compared to their five-membered analogues. Consequently, it is reasonable to assume that donoratoms participating in six-membered rings are more prone to decoordination.

Pincer complexes **Mn-2** and **Mn-5** that differ in the size of the P-N chelate ring provided very similar catalytic results with relatively high enantioselectivity (80 and 82% *ee*, respectively) in ADH reactions. In this case, the possible hemilability of the five- and six-membered P-N rings should be compared. Although, there are examples for the hemilabile behavior of the soft phosphorus donor in transition metal pincer-type complexes, they are still extremely rare [52,53,54], especially in the case of manganese [55]. This is in agreement with the expectation that soft donor phosphorus binds strongly to the relatively soft Mn(I) according to HSAB theory [56]. Additionally, in our case the decoordination of phosphorus during the catalytic cycle would certainly result in low enantioselectivities as the presence of the chiral P-N chelate ring is a prerequisite for the successful stereochemical communication between the catalyst and the substrate. Based on the above considerations, the dissociation of P-donor is very unlikely.

Complexes **Mn-3** and **Mn-6** with uncoordinated dimethylaminopropyl side arm gave similar catalytic results to their analogues **Mn-1** and **Mn-4** without pendant N-containing functionality, respectively. The dimethylamino function in **Mn-3** or **Mn-6** is therefore assumed to remain uncoordinated during catalysis. Furthermore, unlike five-membered chelate complexes **Mn-1** and **Mn-3**, the six-membered chelates **Mn-4** and **Mn-6** exhibited no catalytic activity. This trend might be explained by the presence of the apparently more labile six-membered chelate rings. Sortais et al. reported on similar observations when lower catalytic activities and enantioselectivities could be obtained by six-membered chelates than by the corresponding five-membered systems [23,25].

Table 3
Mn-catalyzed asymmetric transfer hydrogenation (ATH) of acetophenone: screening of the catalysts[a]

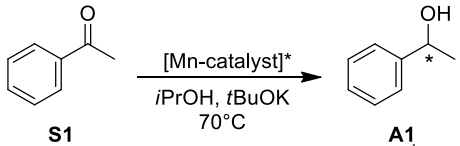

S1 **A1**

Entry	Catalyst	Conversion (%)[b]	*Ee* of **A1** (%)[c]
1	**Mn-1**	91	10 (*R*)
2	**Mn-2**	14	4 (*S*)
3	**Mn-3**	85	8 (*R*)
4	**Mn-4**	0	-
5	**Mn-5**	0	-
6	**Mn-6**	0	-
7[d]	**Mn-1**	90	12 (*R*)
8[e]	**Mn-2**	0	-

[a] Reaction conditions: Catalyst: 0.006 mmol, acetophenone: 0.6 mmol, *t*BuOK: 0.03 mmol, *i*PrOH: 1 ml, temperature: 70°C, reaction time: 24 h. [b]Conversion and chemoselectivity were determined by GC using undecane as internal standard

[c] The *ee* was determined by chiral GC.

[d] EtOH as solvent, in this case the molar ratio of **A1:B1:C1** = 42:44:14.

[e] EtOH as solvent.

2.2.2. Substrate screening and the effect of hydrogen pressure

Encouraged by the high activity and good enantioselectivity achieved by **Mn-2** in the ADH of acetophenone we decided to extend the scope of substrates to evaluate the role of their steric and electronic properties on the catalytic performance (Fig. 6). To this end, ADH of halogen-, methoxy- and trifluoromethyl-substituted acetophenones were studied. Generally, substituted acetophenones could be reduced to the corresponding chiral alcohols with good to excellent enantioselectivities and isolated yields. Interestingly, the electronic properties of the substrates do not affect the *ee* of the catalytic process, similarly good enantioselectivities could be obtained by *m*- and *p*-substituted acetophenone derivatives. It is important to emphasize that the asymmetric hydrogenation of 3,5-bis(trifluoromethyl)acetophenone could also successfully be performed to produce the corresponding fluorinated alcohol, a valuable intermediate for the synthesis of human neurokinin-1 receptor blockers such as Aprepitant [57,58] and Fosaprepitant [59].

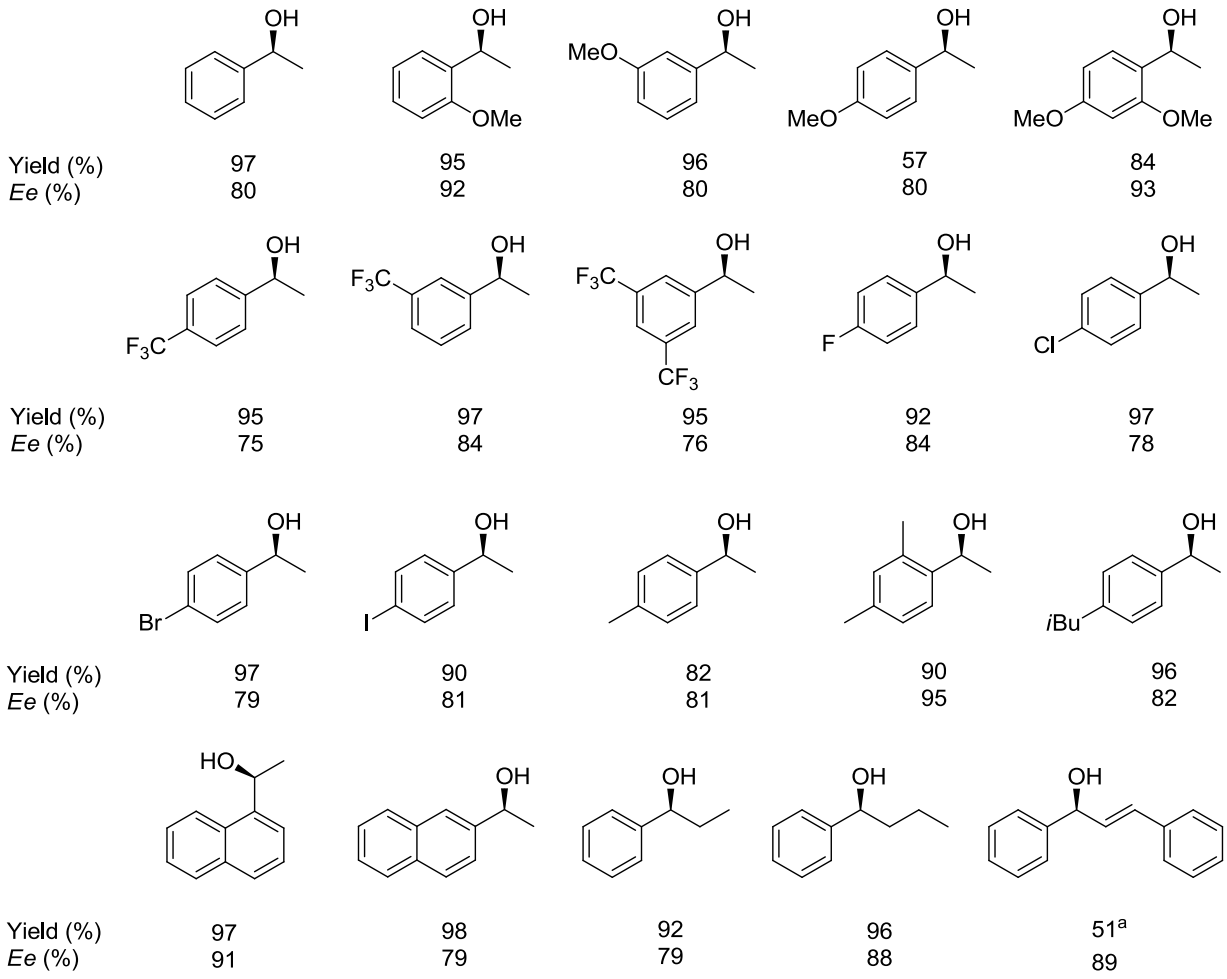

Fig. 6. Chiral alcohols produced in the manganese-catalyzed asymmetric hydrogenation using Mn-2 (Reaction conditions: Catalyst: 0.006 mmol of Mn-2, substrate: 0.6 mmol, *t*BuOK: 0.03 mmol, EtOH: 1 ml, temperature: 50°C, H_2 pressure: 70 bar, reaction time: 20 h. The *ee* was determined by chiral GC or HPLC. The configuration of the dominant product is (*S*). [a]Determined by ^{1}H NMR.

Unlike electronic effects, steric characteristics of the substrates strongly influenced the enantioselectivity. The asymmetric hydrogenation of α-acetonaphthone or acetophenone derivatives containing ring substituents in the *ortho*-position afforded aromatic alcohols with >90% *ee*.

The promising catalytic properties of **Mn-2** in direct hydrogenation reactions motivated us to improve turnover. First, we investigated the effect of the hydrogen pressure on the activity and selectivity in the asymmetric hydrogenation of acetophenone. At a substrate/catalyst molar ratio of 100, the reactions were conducted at 30, 40 and 50 bar H_2-pressures but the reaction time was reduced from 20 to 5 h. As it is shown in Table 4, the conversion steadily increases with the hydrogen pressure under the pressure regime investigated, without the loss of enantioselection (entries 1-3). In order to exploit this effect, the reaction was also performed at 70 and 90 bar at a substrate/catalyst (S/C) molar ratio of 300 (entries 4 and 5). At 90 bar full conversion and 80% *ee* could be obtained after 20 h reaction time. At 70 bar hydrogen pressure, the same outcome was achieved in 30 hours (entry 6). The activity of the catalyst during long reaction times demonstrates its high stability.

2.2.3. Stereochemical and mechanistic considerations

The high selectivity achievable by using catalyst **Mn-2** prompted us to gain a deeper insight into the steric course of the catalytic process. Earlier studies suggest that Mn-H and N-H containing species formed under catalytic conditions serve as active hydrogenating agents in Mn(P,N,N)-catalyzed hydrogenation reactions [27,29]. Based on literature examples [60] and our experimental findings, it is proposed that similar

Table 4
Effect of the hydrogen pressure on catalytic activity and enantioselectivity

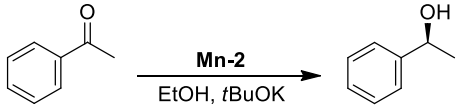

S1 **A1**

Entry	H_2 Pressure (bar)	Conversion (%)[b]	*Ee* of **A1** (%)[c]
1	30	18	81
2	40	32	79
3	50	46	80
4[d]	70	72	81
5[d]	90	>99	81
6[e]	70	>99	81

[a]Reaction conditions: Catalyst: 0.006 mmol **Mn-2**, acetophenone: 0.6 mmol, *t*BuOK: 0.03 mmol, EtOH: 1 mL, temperature: 50°C, reaction time: 5 h.
[b] Conversion and chemoselectivity were determined by GC using undecane as internal standard. The configuration of the prevailing product is (*S*).
[c] The *ee* was determined by chiral GC.
[d] Acetophenone: 1.8 mmol, reaction time: 20 h.
[e] Acetophenone: 1.8 mmol, reaction time: 30 h.

active species are generated from the corresponding bromo-complex **Mn-2** under catalytic conditions (Fig. 7). In the first step, **Mn-2** reacts with *t*BuOK to produce amido-complex **MnA-2**. In the next step, the reaction of **MnA-2** and H_2 results in the formation of hydride species

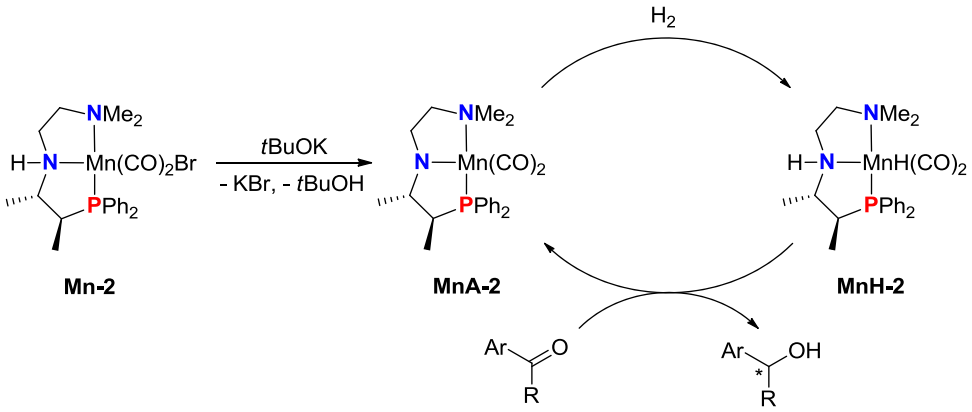

Fig. 7. Proposed catalytic cycle for the asymmetric hydrogenation of prochiral ketones using Mn-2

MnH-2 containing both the Mn-H and N-H functionalities.

When the Mn-H and N-H bonds point in the same direction, an NH…O hydrogen bond forms and the substrate is positioned perpendicularly to the H-Mn-N-H plane so that the carbonyl carbon is oriented above the Mn-H bond [28]. The asymmetric induction arises from the reactivity difference of the substrate's *Re* or *Si* face towards the catalysts [30]. The origin of the differentiation between the enantiotopic faces of the substrate can be assumed to be steric in nature [30,61]. Accordingly, the geometry of catalytically active Mn-H species is crucial in determining enantioselectivity. In order to evaluate the steric factors, we carried out DFT calculations using the CAM-B3LYP functional combination. The SDD basis set/pseudopotential was used for Mn as well as the 6-31G* basis set for the rest of the atoms. Solvent effects of ethanol were taken into account using the CPCM implicit solvation model. It should be emphasized that, according to the metal-ligand bifunctional catalytic model, only those hydride complexes are considered to be catalytically active that have their N-H proton *cis* to the hydride [62]. The geometries and relative energies of three possible structures (**MnH-2A-C**, Fig. 8) were calculated which differ in the chelate ring conformation and/or N-configuration. The calculations showed that the ring conformation and the nitrogen configuration in the lowest-energy hydride species (**MnH-2A**) are identical to those observed experimentally in the solution for the major isomer of complex **Mn-2** (Fig. 5, **I**).

The differentiation between the enantiotopic *Re* and *Si* faces of the ketone by the catalyst presumably rests upon the different steric interaction between the carbonyl substituents (Me or Ph) of the substrate and the axially disposed P-Ph_{ax} ring of the complex (Fig. 9). Intuitively, one expects that out of the two possible substrate orientations to the lowest energy **MnH-2A, MnH-2A(*Re*)** is more favorable than **MnH-2A(*Si*)**, so that the hydride can attack the *Re*-face of the substrate explaining the experimentally observed preferential formation of the (*S*)-product. The steric map [63] of the corresponding Mn-hydride species substantiates this expectation. The application of the same argument to the two higher energy hydride isomers (**MnH-2B** and **MnH-2C**), however, predicts the (*R*)-product as the prevailing enantiomer. As a consequence, the observed (*S*)-selectivity of the catalyst implies that it is the lowest energy hydride (**MnH-2A**) that governs the stereoselection of the process.

3. Conclusions

In conclusion, the Mn(I)-complexes of readily accessible chiral bidentate P,N and potentially tridentate P,N,N ligands have been synthesized and characterized by X-ray crystallography and IR spectroscopy in the solid phase and by using 1D and 2D NMR techniques in solution. The combined spectroscopic analysis of the complexes proved that the length of the N-$(CH_2)_n$-N backbone of P,N,N ligands strongly influences the coordination mode. Compounds with dimethylaminoethyl side chain (n = 2) react with $[Mn(CO)_5Br]$ to form pincer type Mn-complexes, while the dimethylaminopropyl containing systems (n = 3) coordinated to the metal in a bidentate fashion. The coordination pattern of the ligands proved to be crucial in determining their catalytic reactivity. Bidentate systems were more active in ATH reactions while complexes containing ligands coordinated in a tridentate fashion catalyzed the direct hydrogenation of ketonic substrates with high selectivity. Furthermore, it has been established that the size of the P-N chelate ring strongly affects the activity of the catalyst in both ATH and ADH reactions. The most active and enantioselective catalyst **Mn-2** was then applied in the ADH of 20 different substrates where good to excellent enantioselectivities could be obtained. The activity of the catalyst could be enhanced by increasing the hydrogen pressure without the loss of enantioselectivity. In addition, an enantioinduction model has also been proposed for catalyst **Mn-2**.

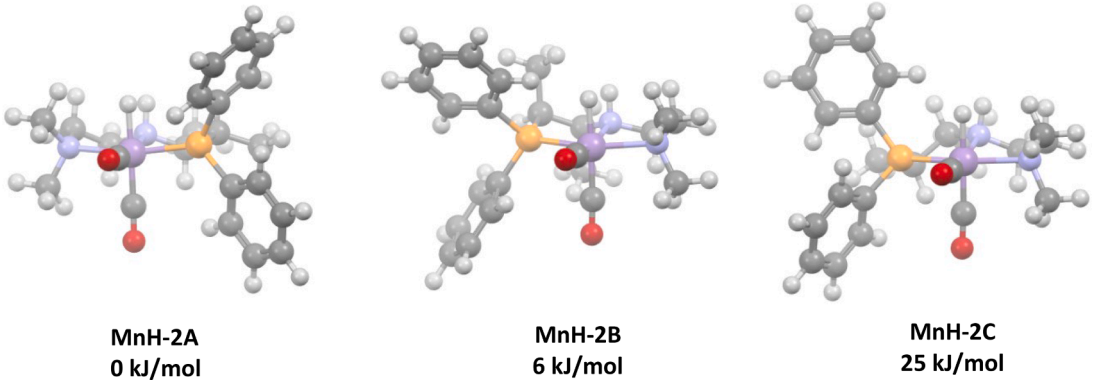

Fig. 8. Optimized geometries and relative entalphies of manganese-hydride complexes containing ligand L2. Atom colors: dark grey – C; light grey – H; purple – Mn; blue -N; yellow – P; red - O.

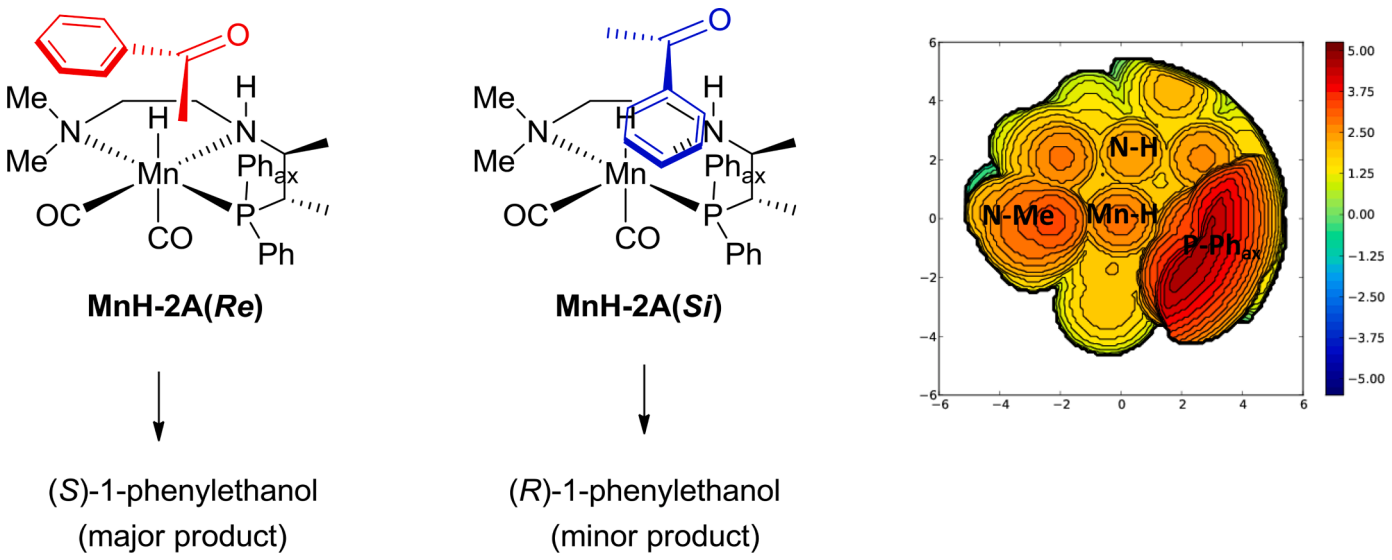

Fig. 9. Analysis of the enantioinduction model by using complex MnH-2A. The right panel shows the steric map of the catalyst.

The remarkable change in the coordination chemistry and the catalytic reactivity by the variation of the tether lengths in alkane-diyl based P,N and P,N,N ligands clearly indicate the high significance of backbone effects in successful catalyst design. This fact together with a working stereoinduction model enables this readily available and highly modular ligand class for further structural fine-tuning to enhance catalytic activity and stereoselectivity. We also believe that these findings can be extrapolated to transition metal catalysts modified by other types of pincer or non-pincer type ligands.

CRediT authorship contribution statement

Zsófia Császár: Methodology, Investigation. **Regina Kovács:** Investigation. **Máté Fonyó:** Investigation. **József Simon:** Investigation. **Attila Bényei:** Conceptualization, Writing – review & editing, Investigation. **György Lendvay:** Conceptualization, Writing – review & editing, Investigation. **József Bakos:** Writing – review & editing, Supervision, Conceptualization. **Gergely Farkas:** Writing – original draft, Supervision, Conceptualization.

Declaration of Competing Interest

The authors declare that they have no known competing financial interests or personal relationships that could have appeared to influence the work reported in this paper.

Data Availability

Data will be made available on request.

Acknowledgements

We thank Mr Béla Édes for skillful assistance in analytical measurements and synthetic experiments. The scientific program was supported by the project NKFIH K128074. This work has been implemented by the TKP2021-NKTA-21 project with the support provided by the Ministry for Innovation and Technology of Hungary from the National Research, Development and Innovation Fund, financed under the 2021 Thematic Excellence Programme funding scheme.

Supplementary materials

Supplementary material associated with this article can be found, in the online version, at doi:10.1016/j.mcat.2022.112531.

References

[1] R.Noyori Ohkuma, Enantioselective ketone and β-Keto Ester hydrogenations (including mechanisms, in: J.G. de Vries, C.J. Elsevier (Eds.), The Handbook of Homogeneous Hydrogenation, Wiley-VCH, Weinheim, 2007, pp. 1105–1163, vol. 3.
[2] N. Arai, T. Ohkuma, Reduction of carbonyl groups: hydrogenation, in: G. A. Molander (Ed.), Science of Synthesis: Stereoselective Synthesis Vol. 2; Stereoselective Reactions of Carbonyl and Imino Groups, Thieme, Stuttgart, 2010, pp. 9–57.
[3] T. Ohkuma, N. Arai, E.M. Carreira, H. Yamamoto, K. Maruoka (Eds.), Comprehensive Chirality, vol. 5, Elsevier, Amsterdam, 2012, pp. 270-300.
[4] H.-U. Blaser, H.-J. Federsel, Asymmetric Catalysis on Industrial Scale: Challenges, Approaches and Solutions, second ed, Wiley-VCH Verlag GmbH & Co. KgaA, Weinheim, 2010.
[5] G.-Q. Chen, X. Zhang, Chapter Four - Metal-catalyzed asymmetric hydrogenation of ketones, Adv. Catal. 68 (2021) 291–339, https://doi.org/10.1016/bs.acat.2021.08.004.
[6] J. Wen, F. Wang, X. Zhang, Asymmetric hydrogenation catalyzed by first-row transition metal complexes, Chem. Soc. Rev. 50 (2021) 3211–3237, https://doi.org/10.1039/D0CS00082E.
[7] L. Alig, M. Fritz, S. Schneider, First-Row Transition Metal (De)Hydrogenation Catalysis Based On Functional Pincer Ligands, Chem. Rev. 119 (2019) 2681–2751, https://doi.org/10.1021/acs.chemrev.8b00555.
[8] F. Agbossou-Niedercorn, C. Michon, Bifunctional homogeneous catalysts based on first row transition metals in asymmetric hydrogenation, Coord. Chem. Rev. 425 (2020), 213523, https://doi.org/10.1016/j.ccr.2020.213523.
[9] K. Das, M.K. Barman, B. Maji, Advancements in multifunctional manganese complexes for catalytic hydrogen transfer reactions, Chem. Commun. 57 (2021) 8534–8549, https://doi.org/10.1039/D1CC02512K.
[10] B. Maji, M.K. Barman, Recent Developments of Manganese Complexes for Catalytic Hydrogenation and Dehydrogenation Reactions, Synthesis 49 (2017) 3377–3393, https://doi.org/10.1055/s-0036-1590818.
[11] E.S. Gulyaeva, E.S. Osipova, R. Buhaibeh, Y. Canac, J.-B. Sortais, D.A. Valyev, Towards ligand simplification in manganese-catalyzed hydrogenation and hydrosilylation processes, Coord. Chem. Rev. 458 (2022), 214421, https://doi.org/10.1016/j.ccr.2022.214421.
[12] M. Garbe, Z. Wei, B. Tannert, A. Spannenberg, H. Jiao, S. Bachmann, M. Scalone, K. Junge, M. Beller, Enantioselective Hydrogenation of Ketones using Different Metal Complexes with a Chiral PNP, Pincer Ligand Adv. Synth. Catal. 361 (2019) 1913–1920, https://doi.org/10.1002/adsc.201801511.
[13] A. Zirakzadeh, S.R.M.M. de Aguiar, B. Stöger, M. Widhalm, K. Kirchner, Enantioselective Transfer Hydrogenation of Ketones Catalyzed by a Manganese Complex Containing an Unsymmetrical Chiral PNP′ Tridentate Ligand, ChemCatChem 9 (2017) 1744–1748, https://doi.org/10.1002/cctc.201700042.
[14] M. Garbe, K. Junge, S. Walker, Z. Wei, H. Jiao, A. Spannenberg, S. Bachmann, M. Scalone, M. Beller, Manganese(I)-Catalyzed Enantioselective Hydrogenation of Ketones Using a Defined Chiral PNP Pincer Ligand, Angew. Chem. Int. Ed. 56 (2017) 11237–11241, https://doi.org/10.1002/anie.201705471.

[15] M.B. Widegren, G.J. Harkness, A.M.Z. Slawin, D.B. Cordes, M.L. Clarke, A Highly Active Manganese Catalyst for Enantioselective Ketone and Ester Hydrogenation Angew, Chem. Int. Ed. 56 (2017) 5825–5828, https://doi.org/10.1002/anie.201702406.

[16] H. Jayaprakash, Mn(i) phosphine-amino-phosphinites: a highly modular class of pincer complexes for enantioselective transfer hydrogenation of aryl-alkyl ketones, Dalton. Trans. 50 (2021) 14115–14119, https://doi.org/10.1039/D1DT02257A.

[17] C.S.G. Seo, B.T.H. Tsui, M.V. Gradiski, S.A.M. Smith, R.H. Morris, Enantioselective direct, base-free hydrogenation of ketones by a manganese amido complex of a homochiral, unsymmetrical P–N–P′ ligand, Catal. Sci. Technol. 11 (2021) 3153–3163, https://doi.org/10.1039/D1CY00446H.

[18] A. Passera, A. Mezzetti, Mn(I) and Fe(II)/PN(H)P Catalysts for the Hydrogenation of Ketones: A Comparison by Experiment and Calculation, Adv. Synth. Catal. 361 (2019) 4691–4706, https://doi.org/10.1002/adsc.201900671.

[19] Z. Wang, X. Zhao, A. Huang, Z. Yang, Y. Cheng, J. Chen, F. Ling, W. Zhong, Manganese catalyzed enantio- and regioselective hydrogenation of α,β-unsaturated ketones using an imidazole-based chiral PNN tridentate ligand, Tetrahedron Lett 82 (2021), 153389, https://doi.org/10.1016/j.tetlet.2021.153389.

[20] F. Ling, H. Hou, J. Chen, S. Nian, X. Yi, Z. Wang, D. Song, W. Zhong, Highly Enantioselective Synthesis of Chiral Benzhydrols via Manganese Catalyzed Asymmetric Hydrogenation of Unsymmetrical Benzophenones Using an Imidazole-Based Chiral PNN Tridentate Ligand, Org. Lett. 21 (2019) 3937–3941, https://doi.org/10.1021/acs.orglett.9b01056.

[21] L. Zhang, Z. Wang, Z. Han, K. Ding, Manganese-Catalyzed anti-Selective Asymmetric Hydrogenation of α-Substituted β-Ketoamides, Angew. Chem. Int. Ed. 59 (2020) 15565–15569, https://doi.org/10.1002/anie.202006383.

[22] C. Liu, M. Wang, S. Liu, Y. Wang, Y. Peng, Y. Lan, Q. Liu, Manganese-Catalyzed Asymmetric Hydrogenation of Quinolines Enabled by π–π Interaction, Angew. Chem. Int. Ed. 60 (2021) 5108–5113, https://doi.org/10.1002/anie.202013540.

[23] K. Azouzi, A. Bruneau-Voisine, L. Vendier, J.-P. Sortais, S. Bastine, Asymmetric transfer hydrogenation of ketones promoted by manganese(I) pre-catalysts supported by bidentate aminophosphines, Catal. Commun. 142 (2020), 106040, https://doi.org/10.1016/j.catcom.2020.106040.

[24] L. Wang, J. Lin, Q. Sun, C. Xia, W. Sun, Amino Acid Derived Chiral Aminobenzimidazole Manganese Catalysts for Asymmetric Transfer Hydrogenation of Ketones, ACS Catal 11 (2021) 8033–8041, https://doi.org/10.1021/acscatal.1c00616.

[25] D. Wang, A. Bruneau-Voisine, J.-P. Sortais, Practical (asymmetric) transfer hydrogenation of ketones catalyzed by manganese with (chiral) diamines ligands, Catal. Commun. 105 (2018) 31–36, https://doi.org/10.1016/j.catcom.2017.10.028.

[26] G.-Y. Zhang, S.-H. Ruan, Y.-Y. Li, J.-X. Gao, Manganese catalyzed asymmetric transfer hydrogenation of ketones, Chin. Chem. Lett. 32 (2021) 1415–1418, https://doi.org/10.1016/j.cclet.2020.10.023.

[27] M.B. Widegren, M.L. Clarke, Towards practical earth abundant reduction catalysis: design of improved catalysts for manganese catalysed hydrogenation, Catal. Sci. Technol. 9 (2019) 6047–6058, https://doi.org/10.1039/C9CY01601E.

[28] L. Zhang, Y. Tang, Z. Han, K. Ding, Lutidine-Based Chiral Pincer Manganese Catalysts for Enantioselective Hydrogenation of Ketones, Angew. Chem. Int. Ed. 58 (2019) 4973–4977, https://doi.org/10.1002/anie.201814751.

[29] K.Z. Demmans, M.E. Olson, R.H. Morris, Asymmetric Transfer Hydrogenation of Ketones with Well-Defined Manganese(I) PNN and PNNP Complexes, Organometallics 37 (2018) 4608–4618, https://doi.org/10.1021/acs.organomet.8b00625.

[30] L. Zeng, H. Yang, M. Zhao, J. Wen, J.H.R. Tucker, X. Zhang, *C1*-Symmetric PNP Ligands for Manganese-Catalyzed Enantioselective Hydrogenation of Ketones: Reaction Scope and Enantioinduction Model, ACS Catal 10 (2020) 13794–13799, https://doi.org/10.1021/acscatal.0c04206.

[31] Z.H. Wang, M.R. Eberhard, C.M. Jensen, S. Matsukawa, Y. Ymamoto, A structure–activity relationship for pincer palladium(II) complexes — influence of ring-size of metallacycles on the activity in allylic alkylation, J. Organomet. Chem. 681 (2003) 189–195, https://doi.org/10.1016/S0022-328X(03)00604-1.

[32] G. Mancano, M.J. Page, M. Bhadbhade, B.A. Messerle, Hemilabile and Bimetallic Coordination in Rh and Ir Complexes of NCN Pincer Ligands, Inorg. Chem. 53 (2014) 10159–10170, https://doi.org/10.1021/ic501158x.

[33] R. Linder, B. van den Bosch, M. Lutz, J.N.H. Reek, J.I. van der Vlugt, Tunable Hemilabile Ligands for Adaptive Transition Metal Complexes, Organometallics 30 (2011) 499–510, https://doi.org/10.1021/om100804k.

[34] P.A. Dub, B.L. Scott, J.C. Gordon, Air-Stable NNS (ENENES) Ligands and Their Well-Defined Ruthenium and Iridium Complexes for Molecular Catalysis, Organometallics 34 (2015) 4464–4479, https://doi.org/10.1021/acs.organomet.5b00432.

[35] J.A. Fuentes, S.M. Smith, M.T. Scharbert, I. Carpenter, D.B. Cordes, A.M.Z. Slawin, M.L. Clarke, On the Functional Group Tolerance of Ester Hydrogenation and Polyester Depolymerisation Catalysed by Ruthenium Complexes of Tridentate Aminophosphine Ligands, Chem. Eur. J. 21 (2015) 10851–10860, https://doi.org/10.1002/chem.201500907.

[36] G. Farkas, Z. Császár, K. Stágel, E. Nemes, S. Balogh, I. Tóth, A. Bényei, G. Lendvay, J. Bakos, Efficient stereochemical communication in phosphine-amine palladium-complexes: Exploration of N-substituent effects in coordination chemistry and catalysis, J. Organomet. Chem. 846 (2017) 129–140, https://doi.org/10.1016/j.jorganchem.2017.04.033.

[37] Z. Császár, E.Z. Szabó, A.C. Bényei, J. Bakos, G. Farkas, Chelate ring size effects of Ir(P,N,N) complexes: Chemoselectivity switch in the asymmetric hydrogenation of α,β-unsaturated ketones, Catal. Commun. 146 (2020), 106128, https://doi.org/10.1016/j.catcom.2020.106128.

[38] R. vanPutten, E.A. Uslamin, M. Garbe, C. Liu, A. Gonzalez-de-Castro, M. Lutz, K. Junge, E.J.M. Hensen, M. Beller, L. Lefort, E.A. Pidko, Non-Pincer-Type Manganese Complexes as Efficient Catalysts for the Hydrogenation of Esters, Angew. Chem. Int. Ed. 56 (2017) 7531–7534, https://doi.org/10.1002/anie.201701365.

[39] W. McFarlane, J.D. Swarbrick, J.L. Bookham, An NMR study of the solution conformations of di(tertiary phosphine) complexes of orthopalladated 1-phenyl-1-(N,N-dimethylamino)ethane, J. Chem. Soc., Dalton. Trans. (1998) 3233–3238, https://doi.org/10.1039/A806313C.

[40] N.A. Espinosa-Jalapa, A. Kumar, G. Leitus, Y. Diskin-Posner, D. Milstein, Synthesis of Cyclic Imides by Acceptorless Dehydrogenative Coupling of Diols and Amines Catalyzed by a Manganese Pincer Complex, J. Am. Chem. Soc. 139 (2017) 11722–11725, https://doi.org/10.1021/jacs.7b08341.

[41] N.A. Espinosa-Jalapa, A. Nerush, L.J.W. Shimon, G. Leitus, L. Avram, Y. Ben-David, D. Milstein, Manganese-Catalyzed Hydrogenation of Esters to Alcohols, Chem. Eur. J. 23 (2017) 5934–5938, https://doi.org/10.1002/chem.201604991.

[42] M. Peña-López, P. Piehl, S. Elangovan, H. Neumann, M. Beller, Manganese-Catalyzed Hydrogen-Autotransfer C−C Bond Formation: α-Alkylation of Ketones with Primary Alcohols, Angew. Chem. Int. Ed. 55 (2016) 14967–14971, https://doi.org/10.1002/anie.201607072.

[43] K.R. Rohit, S. Radhika, S. Saranya, G. Anilkumar, Manganese-Catalysed Dehydrogenative Coupling – An Overview, Adv. Synth. Catal. 362 (2020) 1602–1650, https://doi.org/10.1002/adsc.201901389.

[44] J.A. Fuentes, S.M. Smith, M.T. Scharbert, I. Carpenter, D.B. Cordes, A.M.Z. Slawin, M.L. Clarke, On the Functional Group Tolerance of Ester Hydrogenation and Polyester Depolymerisation Catalysed by Ruthenium Complexes of Tridentate Aminophosphine Ligands, Chem. Eur. J. 21 (2015) 10851–10860, https://doi.org/10.1002/chem.201500907.

[45] W. Baratta, M. Ballico, G. Esposito, P. Rigo, Role of the NH_2 Functionality and Solvent in Terdentate CNN Alkoxide Ruthenium Complexes for the Fast Transfer Hydrogenation of Ketones in 2-Propanol, Chem. Eur. J. 14 (2008) 5588–5595, https://doi.org/10.1002/chem.200701870.

[46] Z. Freixa, P.W.N.M. van Leeuwen, Bite angle effects in diphosphine metal catalysts: steric or electronic? Dalton Trans (2003) 1890–1901, https://doi.org/10.1039/B300322C.

[47] X. Fang, M. Sun, J. Zheng, B. Li, L. Ye, X. Wang, Z. Cao, H. Zhu, Y. Yuan, CH_2 Linkage Effects on the Reactivity of Bis(aminophosphine)–Ruthenium Complexes for Selective Hydrogenation of Esters into Alcohols, Sci. Rep. 7 (2017) 3961, https://doi.org/10.1038/s41598-017-04362-9.

[48] D.W. Allen, B.F. Taylor, The chemistry of heteroarylphosphorus compounds. Part 15. Phosphorus-31 nuclear magnetic resonance studies of the donor properties of heteroarylphosphines towards selenium and platinum(II), J. Chem. Soc., Dalton Trans (1982) 51–54, https://doi.org/10.1039/DT9820000051.

[49] G. Farkas, S. Balogh, J. Madarász, Á. Szöllősy, F. Darvas, L. Ürge, M. Gouygou, J. Bakos, Phosphine–phosphite ligands: chelate ring size vs. activity and enantioselectivity relationships in asymmetric hydrogenation, Dalton Trans 41 (2012) 9493–9502.

[50] P. Braunstein, F. Naud, Hemilability of Hybrid Ligands and the Coordination Chemistry of Oxazoline-Based Systems, Angew. Chem. Int. Ed. 40 (2001) 680–699, https://doi.org/10.1002/1521-3773(20010216)40:4<680::AID-ANIE6800>3.0.CO;2-0.

[51] E Peris, R.H. Crabtree, Key factors in pincer ligand design, Chem. Soc. Rev. 47 (2018) 1959–1968, https://doi.org/10.1039/C7CS00693D.

[52] D.P. Krut'ko, M.V. Borzov, E.N. Veksler, A.V. Churakov, K. Mach, Crystal structures and solution dynamics of monocyclopentadienyl titanium (IV) complexes bearing pendant ether and phosphanyl type functionalities, Polyhedron 22 (2003) 2885–2894, https://doi.org/10.1016/S0277-5387(03)00407-8.

[53] L. Yong, E. Hofer, R. Wartchow, H. Butenschön, Oxidative addition of hydrosilanes, hydrogermane, and hydrostannane to cyclopentadienylcobalt (I) bearing a pendant phosphane ligand: cyclopentadienylhydridocobalt (III) chelate complexes with silyl, germyl, and stannyl ligands. Organometallics 22 (2003), 5463–5467. https://doi.org/10.1021/om030581b.

[54] X.-J. Yu, H.-Y. He, L. Yang, H.-Y. Fu, X.-L. Zheng, H. Chen, R.-X. Li, Hemilabile N-heterocyclic carbene (NHC)-nitrogen-phosphine mediated Ru (II)-catalyzed N-alkylation of aromatic amine with alcohol efficiently, Catal. Commun. 95 (2017) 54–57, https://doi.org/10.1016/j.catcom.2017.03.007.

[55] W. Yang, I. Yu. Chernyshov, R.K.A. van Schendel, M. Weber, C. Müller, G. A. Filonenko, E.A. Pidko, Robust and efficient hydrogenation of carbonyl compounds catalysed by mixed donor Mn(I) pincer complexes, Nat. Commun. 12 (2021) 12, https://doi.org/10.1038/s41467-020-20168-2.

[56] L.-N. Ji, M.E. Rerek, F. Basolo, Kinetics and Mechanism of Substitution Reactions of $Mn(\eta^5\text{-}C_9H_7)(CO)_3$ and $Mn(\eta^5\text{-}C_{13}H_9)(CO)_3$, Organometallics 3 (1984) 740–745, https://doi.org/10.1021/om00083a016.

[57] K.M.J. Brands, J.F. Payack, J.D. Rosen, T.D. Nelson, A. Candelario, M.A. Huffman, M.M. Zhao, J. Li, B. Craig, Z.G.J. Song, D.M. Tschaen, K. Hansen, P.N. Devine, P. J. Pye, K. Rossen, P.G. Dormer, R.A. Reamer, C.J. Welch, D.J. Mathre, N.N. Tsou, J. M. McNamara, P.J. Reider, Efficient Synthesis of NK_1 Receptor Antagonist Aprepitant Using a Crystallization-Induced Diastereoselective Transformation, J. Am. Chem. Soc. 125 (2003) 2129–2135, https://doi.org/10.1021/ja027458g.

[58] M.M. Zhao, J.M. McNamara, G.J. Ho, K.M. Emerson, Z.J. Song, D.M. Tschaen, K. M. Brands, U.H. Dolling, E.J. Grabowski, P.J. Reider, I.F. Cottrell, M.S. Ashwood, B. C. Bishop, Practical Asymmetric Synthesis of Aprepitant, a Potent Human NK-1 Receptor Antagonist, via a Stereoselective Lewis Acid-Catalyzed Trans Acetalization Reaction, J. Org. Chem. 67 (2002) 6743–6747, https://doi.org/10.1021/jo0203793.

[59] C.P. Dorn, J.J. Hale, M. MacCoss, S.G. Mills, Preparation of morpholine tachykinin receptor antagonist prodrugs. WO9523798A1, 1995.
[60] Y. Wang, M. Wang, Y. Li, Q. Liu, Homogeneous manganese-catalyzed hydrogenation and dehydrogenation reactions, Chem 7 (2021) 1180–1223, https://doi.org/10.1016/j.chempr.2020.11.013.
[61] I.D. Gridnev, P.A. Dub, Enantioselection in Asymmetric Catalysis, CRC Press, Boca Raton, London, New York, 2017.
[62] P.A. Dub, J.C. Gordon, The role of the metal-bound N–H functionality in Noyori-type molecular catalysts, Nat. Rev. Chem. 2 (2018) 396–408, https://doi.org/10.1038/s41570-018-0049-z.
[63] A. Poater, F. Ragone, R. Mariz, R. Dorta, L. Cavallo, Comparing the Enantioselective Power of Steric and Electrostatic Effects in Transition-Metal-Catalyzed Asymmetric Synthesis, Chem. Eur. J. 16 (2010) 14348–14353, https://doi.org/10.1002/chem.201001938.